Rigorous Beam Propagation Analysis of Tapered Spot-Size Converters in Deep-Etched Semiconductor Waveguides

B. M. A. Rahman, *Senior Member, IEEE*, W. Boonthittanont, S. S. A. Obayya, T. Wongcharoen, E. O. Ladele, and K. T. V. Grattan

***Abstract*—A rigorous study of a tapered spot-size converter in a deep-etched GaAs/AlGaAs optical modulator is reported through the use of full vectorial approaches. Mode beating in the tapered section, the expansion of the spot-size, and the consequent enhancement of the coupling to an optical fiber are also reported.**

***Index Terms*—Beam propagation method, finite-element method, optical coupling, spot-size converters.**

I. Introduction

In the design of semiconductor optical waveguides, power splitters, bends, lasers, modulators, and amplifiers, two different manufacturing technologies creating different design approaches are often used. The first type, the shallow rib type designs [1], [2], are more widely used; however, the performance of the devices often critically depends on the etch depth, and in this approach, the resulting optical mode shape is also difficult to control. On the other hand, by deep-etching through and beyond the core to part of the lower cladding [3], the modal behavior of the structure would be less sensitive to the etch depth. Besides, due to the strong horizontal confinement, the bending losses would be greatly reduced [4], [5] and consequently a more compact optoelectronic system design would be possible, which will lead to an increased functionality of the subsystems than would be allowed by using the shallow-etching approach. This type of deep-etched waveguide structure has been used for the design of multimode interference (MMI)-based power splitters [6], [7], delay lines, and high-speed modulators [8].

For many semiconductor devices, such as lasers, modulators, and amplifiers, their optical spot-sizes are small in size and often highly nonsymmetrical. If such a device is directly butt-coupled to a single-mode fiber (SMF), which has a much larger and circular field profile, often 90% or more of the optical power would be lost due to the mismatch between their field profiles. In the design of a deep-etched semiconductor waveguide, effectively single-mode operation is possible [3] for a much wider waveguide by controlling the lower cladding index to radiate out all the higher order modes. In this case, the resulting spot-size is slightly bigger and more symmetrical, but not yet comparable with that of a SMF. As an example, in the design optimization of high-speed GaAs modulators [8], often values of the waveguide core width of between 3.0 to 5.0 μm with heights between 1.5 to 3.0 μm are used, which may yield 30-40% coupling efficiency. However, these spot-sizes need to be improved further to reduce significantly the coupling loss with the SMFs and to minimize the packaging costs.

Recently, in the design of a semiconductor photonic component or a subsystem, monolithically integrated spot-size converters (SSCs) have often been incorporated to improve the coupling efficiency along with the much relaxed alignment tolerances. In the design of such an SSC, often the primary guide is tapered down [9]–[13] to push the mode to the secondary guide, which is designed to have a similar spot-size to that of a SMF. In this work, a SSC converter compatible with deep-etched semiconductor photonic components is investigated, by using rigorous vectorial approaches to study the spot-size transformation and the resultant enhancement of the coupling efficiency.

II. Numerical Method

The expansion of the spot-size is often achieved by reducing the core dimension to a sufficiently small value [9]–[13] so that the primary guide cannot support any guided mode and consequently the optical power is pushed out of this core to a secondary core. Often a closely spaced twin-core superstructure may be used, with one core being axially nonuniform and the resultant waveguide cross-section can be quite complex in shape. To study the mode-shape and the evolution of the optical beam, both a modal solution and a beam propagation-type evolutionary approach would be necessary. Over the last two decades, many numerical methods have been reported for the eigenmode solutions of the optical waveguides. However, many of these approaches would not be accurate for optical waveguides operating near their modal cutoff conditions. In this respect, the **H**-field based full-vectorial finite-element method (FEM) [14] has established itself as one of the most rigorous full vectorial approaches for the characterization of a wide range of optical waveguides [14], [15]. In the FEM approach, the waveguide cross section is represented by a large number of triangles, and since these triangles could be of different shapes and sizes, any waveguide cross-section can be accurately represented. The full vectorial **H**-field formulation (VFEM) is used here, which allows each of these elements to have different

Manuscript received May 29, 2003; revised September 3, 2003. This work was supported by EPSRC.

B. M. A. Rahman, W. Boonthittanont, S. S. A. Obayya, E. O. Ladele, and K. T. V. Grattan are with the School of Engineering and Mathematical Sciences, City University London, EC1V 0HB London, U.K. (e-mail: B.M.A.Rahman@city.ac.uk).

T. Wongcharoen is with Bangkok University, Bangkok, Thailand.

Digital Object Identifier 10.1109/JLT.2003.821753

material properties—for example, being linear or nonlinear, being lossless or with material loss or gain, and being isotropic, anisotropic, or electrooptic—and so the eigenmodes of any practical guided-wave devices can be accurately obtained. The VFEM approach has been used to obtain the modal solutions of linear, nonlinear, diffused, anisotropic, passive, and active optical waveguides and have also been particularly used in the designs of SSCs [9]–[11], [16].

Similarly, to study the transformation of the spot-size through a tapered guided-wave structure, the beam propagation method (BPM) [11]–[13] is also required. To reduce the computational time, often a scalar or semivectorial [11] formulation has been used or one of the transverse dimensions has been reduced [10] by using the effective index method, which unfortunately also reduces the solution accuracy. In this respect, the finite-element-based BPM has been shown to be accurate and numerically efficient with the use of irregular meshes. An important advantage of this work is that most of the commercial BPM codes are based on the finite difference approach, which is numerically less efficient. In this paper, a full vectorial and fully three-dimensional FEM-based BPM [17] incorporating a nonparaxial wide-angle approach and the perfectly matched layer (PML) around the computational window is considered. Finally the overlap method [12] has been used to calculate the coupling efficiency between the expanded optical beam at the end of the SSC and the SMF.

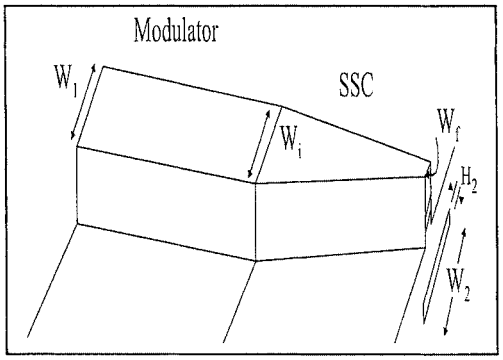

(a)

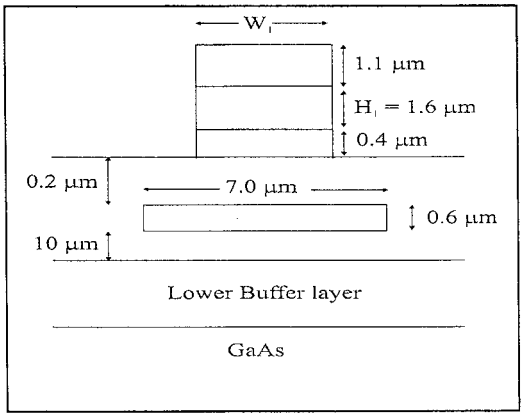

(b)

Fig. 1. Schematic diagram of a spot-size converter (a) incorporating a tapered core and (b) its cross-section.

III. Results

In this paper, the spot-size conversion of a high-speed GaAs electrooptic modulator section is undertaken. In the monolithically integrated SSC section, as shown in Fig. 1(a), the upper core width is gradually reduced, which is much easier to fabricate by using standard processing techniques, to bring this guide below its cutoff value. A parallel secondary lower guide is designed inside the spacer region to have a larger spot-size than the primary upper guide to collect the optical energy, when the upper guide reaches its modal cutoff condition. The cross-section of the SSC structure is shown in Fig. 1(b). The upper cladding, the core, and the lower cladding thickness are taken as 1.1, 1.6, and 0.4 μm, respectively. The width of the primary guide in the modulator section is set to 4.0 μm, and this upper guide is tapered in the SSC section. The refractive indexes for the upper cladding, core, lower cladding, and spacer layer are taken as 3.2323, 3.3769, 3.3293, and 3.3532, respectively, at the operating wavelength of 1.55 μm. The whole structure may be grown on a semi-insulating GaAs substrate. In this design, the width of the lower guide (W_2) is assumed to be 7.0 μm, which gives a horizontally expanded spot-size similar to that of an SMF. For this lower secondary guide, a thicker 10-μm lower cladding is used to allow adequate vertical expansion of the optical beam but a thinner 0.2-μm spacer layer is used to facilitate power coupling from the upper primary guide. The core thickness of the secondary guide (H_2) is adjusted, such that this guide also operates very close to its modal cutoff. For a core thickness of 0.6 μm with its core index 3.3769, the vertical spot-size of this guide has been calculated to be nearly 5.0 μm. This value is slightly smaller than that of an SMF, but a further expanded spot-size is not sought at this stage as otherwise the total spacer layer thickness would also have to be increased significantly to accommodate such a large mode profile. The leakage losses for the optical modes can be controlled by proper design of the lower cladding and the spacer layer, and a properly designed guide could effectively be a single-moded guide.

To obtain the supermode profiles of the SSC with the laterally tapered upper core W_1, the complete coupled superstructure is considered. More than 20 000 first-order irregularly sized triangular elements have been considered to represent the structure, and the VFEM [14] is used to obtain the modal solutions. The variation of the spot-size with the upper core width W_1 is shown in Fig. 2. It can be observed that the horizontal spot-size σ_x, as shown by a dashed line, is initially reduced as the width is reduced. However, when the primary guide is narrow enough, and cannot support a guided mode any further—or, in other words, as the cutoff is reached—the mode shape expands rapidly. On the other hand, it can be observed that the vertical spot-size σ_y, as shown by a solid line, remains stable (as its height H_1 was not varied) until the cutoff is reached, when this also expands rapidly. In this case, the spot-size has been defined as the distance from one side to the other (full width) of the waveguide, where the field intensity is reduced to $1/e^{\text{th}}$ of the maximum intensity (i.e., the power intensity is $1/e^2$). The expansion of the overall spot-size area σ_A is also shown by a dashed-dotted line. Here the spot-size area is defined as the area where field intensity is greater than $1/e$ of its maximum strength.

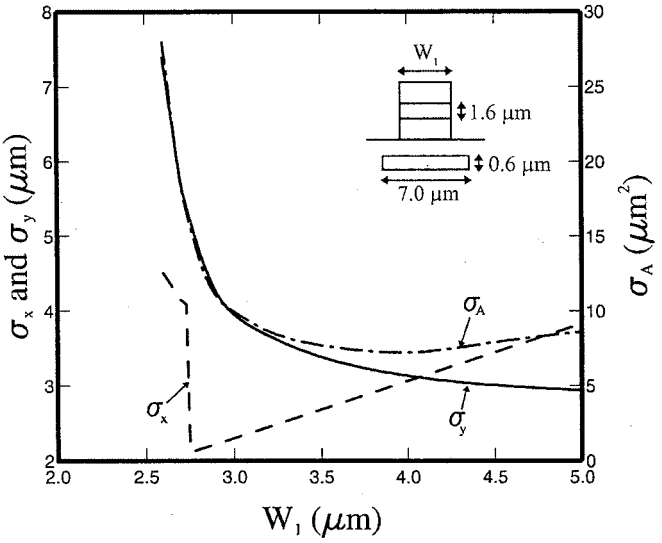

Fig. 2. Variation of the spot-size with the upper core width, W_1, using the VFEM modal solution.

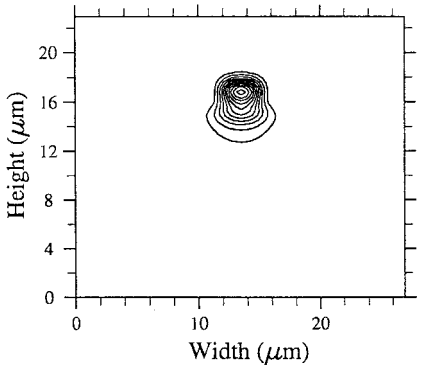

(a)

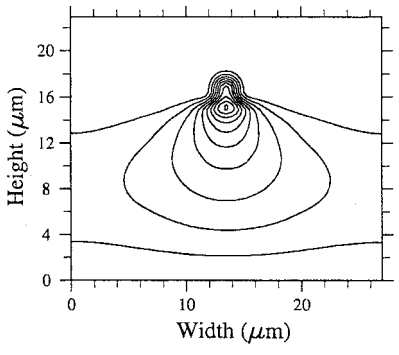

(b)

Fig. 3. The dominant H_y field profile of the fundamental quasi-TE mode for a uniform coupled waveguide, for an upper waveguide width (a) 4.0 μm and (b) 2.6 μm.

The dominant field profiles H_y for the fundamental quasi-TE mode (H_y^{11}) are shown in Fig. 3(a) and (b) for the upper waveguide width (W_1), 4.0 μm, and 2.6 μm, respectively. It can be observed that the mode-shape of the modulator section (when $W_1 = 4.0\,\mu$m) is well confined to enhance the overlap between the optical and the modulating fields. However, this field, being smaller in size, would not be very suitable for directly coupling to a SMF. On the other hand, the mode shape at $W_1 = 2.6\,\mu$m is more significantly expanded and would be more suitable to couple to a SMF.

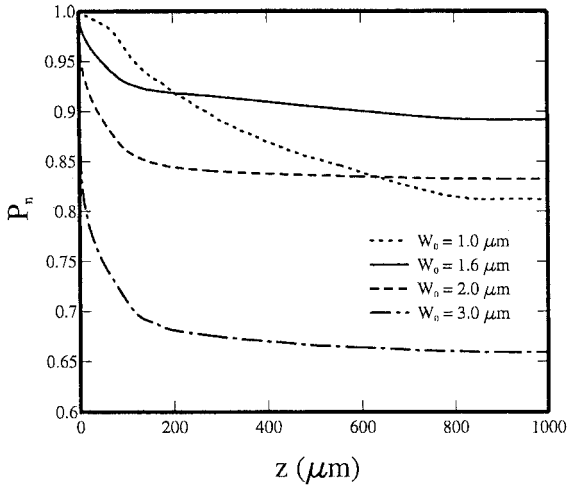

Fig. 4. Variation of the total guided power along a uniform waveguide when an arbitrary Gaussian profile beam is launched, for different mode-size radii, Ω.

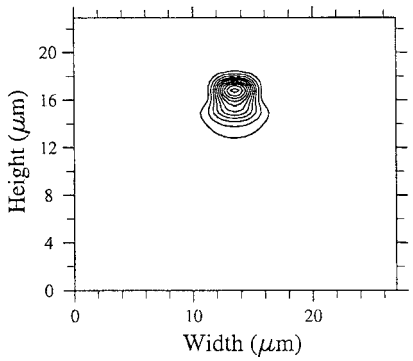

Fig. 5. The output H_y field profile at $z = 1000\ \mu$m, obtained by using the BPM approach, when a Gaussian beam with $\Omega = 1.6\ \mu$m is launched into a uniform guide with $W_1 = 4.0\ \mu$m.

However, to study the evolution of the optical beam, a BPM-type approach is necessary. In this paper, a full vectorial FEM-based BPM [17] is used to study the spot-size conversion along the tapered structure. Initially the stability of the BPM was tested by launching either the mode shape obtained by the VFEM or an arbitrary Gaussian beam into a uniform structure. When the VFEM mode shape is used as the excitation, the propagating beam quickly settles to the same mode shape without shedding any power (as the input field profile by FEM is almost the same as that which would be supported by the structure). However, when a Gaussian beam is launched, depending on its mode size, the optical beam would settle into the proper guided mode after radiating the higher order modes, which were also excited. Variations of the optical power, normalized to the input power along the propagation distance z, are shown in Fig. 4 for various Gaussian radii Ω_0. It can be observed that when Ω_0 is 1.6 μm, the total power loss was minimum as this size was closer to the mode size, which can be guided by this structure. The resulting beam shape is shown in Fig. 5, which shows a very close resemblance to the mode shape shown in Fig. 3(a), which was obtained by using the VFEM.

Next, the evolution of the optical beam along a tapered structure is shown in Fig. 6. In this case the initial width (W_i) and

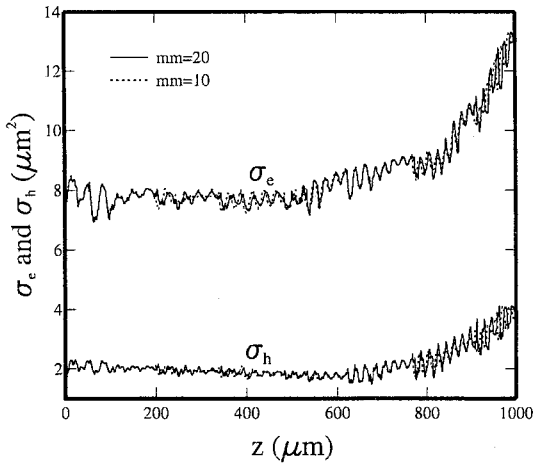

Fig. 6. Variations of the half-power spot-size (σ_h) and $1/e$ intensity spot-size (σ_e) for 1000 μm long tapered SSC with two different remeshing schemes.

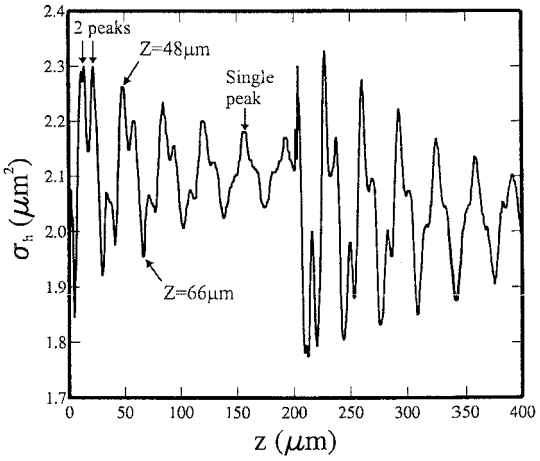

Fig. 7. Variation of the half-power spot-size σ_h along the waveguide with an abrupt discontinuity.

the final width (W_f) were 4.0 and 2.6 μm, respectively. Initially the length of the tapered SSC section (L) was considered to be 1000 μm. In the BPM analysis, the z-step size was taken as 0.5 μm, after exploiting the wide-angle nonparaxial approach. As the cross-section of the SSC is continuously changing, the mesh has to be regenerated along the axial direction. In the BPM approach, mesh generation (along with the evaluation of the matrices) takes more CPU time than z-stepping, so it was decided to remesh only at a given interval *mm*. In reality, also due to the mask design process, the waveguide width would not also be continuously varied but occur in many smaller steps.

Variations of the spot-sizes for the remeshing step, $mm = 10$ and 20, are shown by dotted and solid lines, respectively. For $mm = 10$, remeshing was carried out at every 5 μm, so in total 200 lateral steps of 7 nm each were considered to represent the above tapered structure. Besides the value of σ_e, information about the half-power spot-size (σ_h) might also be useful; hence both σ_e and σ_h are plotted in this figure. It can be observed that σ_e (with up to 14% of the maximum power intensity) has a larger area than the σ_h, covering 50% of the maximum power intensity. It can also be observed that initially the spot-size reduces and subsequently increases along the axial direction as the width of the primary core is reduced. However, it should be noted that the spot-size area σ_e has expanded only up to 12–14 μm^2, rather than 25 μm^2, as shown in Fig. 2 for the same final width $W_f = W_1 = 2.6$ μm. The reason for the smaller expansion will be considered later. However, it can also be noticed that the spot-size goes through some small oscillations, and this will be addressed in the next section.

Most of the published work on tapered spot-size converters has reported on the resulting expansion of the spot-size, but very few authors have explicitly reported such oscillations. In some work, a closer inspection can identify such oscillations, such as was reported by Visrikata *et al.* [13] and Balmer *et al.* [18]. The authors are aware that this is clearly due to the change in the axial direction, and to test this, an abrupt junction in the waveguide is considered and a more detailed investigation is carried out. Fig. 7 shows the variation of the σ_h with the axial distance, when the width is abruptly changed from 4.0 to 3.3 μm at $z = 200$ μm. Two groups of damped oscillations can

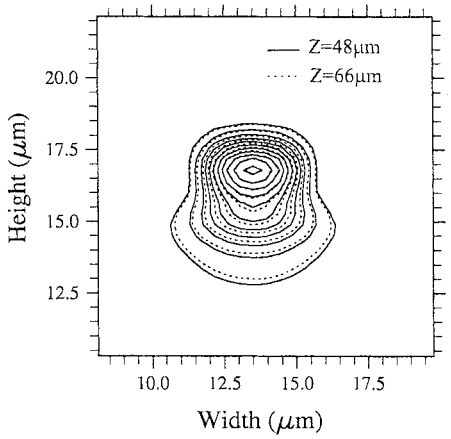

Fig. 8. Dominant H_y field profiles at $z = 48$ and 66 μm, along a waveguide with an abrupt discontinuity.

be observed: one starting at $z = 0$ μm, when the input field is trying to settle to the mode field, and again at $z = 200$ μm, when the waveguide width is abruptly reduced. It can be noted that at the start of the oscillations, two peaks are clearly visible, due to interference between the fundamental mode and the two higher order modes. Since the third mode radiates quickly (as its leakage loss is higher), after a while only the mode beating between the fundamental and the second mode is visible, which also shows that its amplitude is continuously being reduced. The beat length roughly correlates with the difference between their propagation constants, which clearly proves that the modal interference is the main reason for these spot-size fluctuations, and other numerical parameters play insignificant roles. It can also be noted that the average spot-size for $W_1 = 3.6$ μm (right half) is smaller than that for $W_1 = 4.0$ μm (left half), as would be expected. The resulting absolute values of the dominant field H_y are shown at $z = 48$ and 66 μm, respectively, in Fig. 8. It can be noted that the field variation at these two positions is rather small, compared to the rather larger variations in their spot-sizes at these two positions, as shown in Fig. 7. The larger variation in the spot-size could be due to the modal and spatial phase variations and may also be due to the contribution from the nondominant field components.

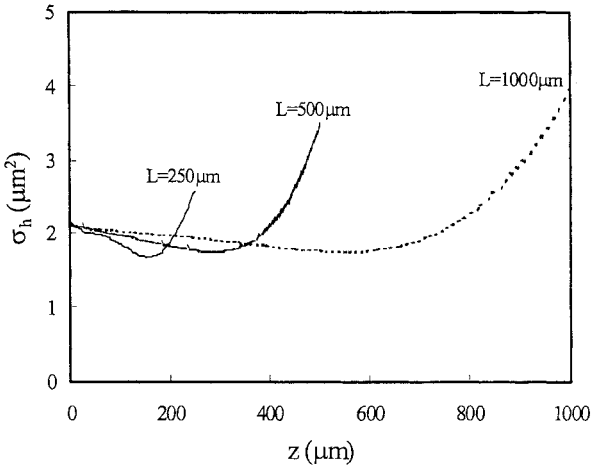

Fig. 9. Variation of the half-power spot-size ($\sigma_{\rm h}$) along the axial direction for the final width $W_{\rm f} = 2.6\ \mu$m but with different tapered lengths L.

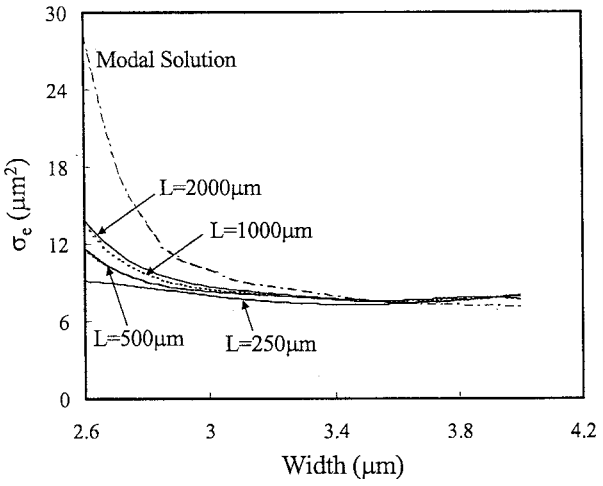

Fig. 10. Variation of the spot-size $\sigma_{\rm e}$, with the local waveguide width for various tapered lengths L but with a fixed final width $W_{\rm f} = 2.6\ \mu$m.

Earlier, in Fig. 6, it was also observed that the spot-size expansion was rather limited when a 1000-μm-long section was used with the final upper core width $W_{\rm f} = 2.6\ \mu$m. Next, to test the effect of the overall length on the expansion of the spot-size, SSC sections of different length L are considered. The variations of $\sigma_{\rm h}$ with the axial distance are shown for 250-, 500-, and 1000-μm-long SSCs in Fig. 9. It can be noted that in all the cases, initially the spot-size is reduced, as expected, then expanded: however, their final spot-sizes are quite different. It should be noted that mode expansion occurs only when the waveguide approaches its modal cutoff. However, for a shorter taper, the structure is not long enough for the evolving beam to take the shape of the mode profile supported by the terminating width $W_{\rm f}$. This is the reason that, as a longer SSC is used, the mode expansion comes closer to the value indicated by the modal solutions. Similar observations were reported by Kobayashi *et al.* [12] on the effect of the tapered length on the mode-size expansion for a fixed waveguide thickness ratio.

The variations of the spot-size $\sigma_{\rm e}$ with the local width, for various tapered lengths are shown in Fig. 10. It can be observed that the spot-size increases as the waveguide width is reduced, but this expansion is not as rapid as was indicated by their modal solutions (as shown in Fig. 2) and also strongly depends on the device length. For a longer device, the spot-size expansion is larger for a given waveguide width, as a slow taper allows adequate expansion. However, it can also be observed that the spot-size is significantly smaller than that indicated by a rigorous modal solution, even when the SSC is 2000 μm in length. This indicates that, in practice, for a compact SSC, the final taper width has to be much smaller than the value indicated by their modal solutions.

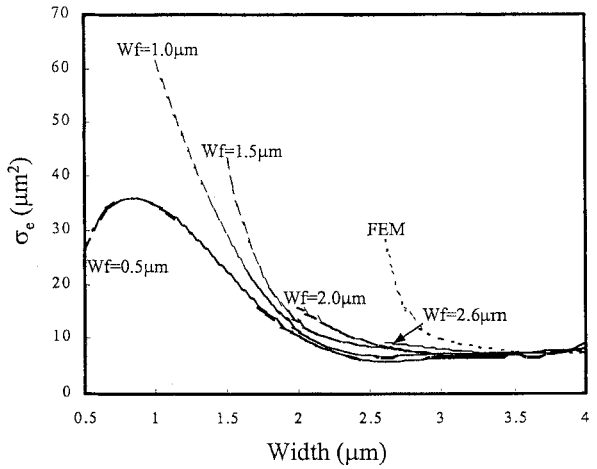

Fig. 11. Variation of the spot-size $\sigma_{\rm e}$, with the local upper waveguide width for different final widths $W_{\rm f}$, when the SSC length is 250 μm.

Next, the effect of the final width for a 250-μm-long SSC is studied. Variations of $\sigma_{\rm h}$ with the local width, for various final widths ($W_{\rm f}$), are shown in Fig. 11. It can be noted that for a 250-μm-long device, when the final width is reduced to 1.5 μm, the spot-size expansion is considerably larger than that of $W_{\rm f} = 2.6\ \mu$m, which is also shown. The spot-size obtained by the VFEM modal solution is also shown in this figure for comparison. It can be noted that for $W_{\rm f} = 1.0\ \mu$m, the expansion is rather larger than necessary for its coupling to a SMF. Similarly, when $W_{\rm f} = 0.5\ \mu$m, the spot-size rather reduces, as in this case the optical beam loses its lateral confinement. The resulting final beam profiles are also shown in Fig. 12(a) and (b) for $W_{\rm f} = 1.5$ and $1.0\ \mu$m, respectively. It can be noted that the beam shape for $W_{\rm f} = 1.0\ \mu$m is of poorer quality, even when spot-size shows a greater enlargement. The existing asymmetry of the field profiles is due to smaller separation distance used between the two waveguide cores.

The final test was carried out to study the coupling efficiency of the resulting beam with an SMF obtained by using the overlap integral method [12]. The radial spot-size (Ω) of the SMF has been taken as 5.5 μm. The variations of the transmittance with the vertical misalignment are shown in Fig. 13 for a tapered SSC with final widths $W_{\rm f} = 1.4, 1.5$, and $1.6\ \mu$m, respectively. For comparison, the coupling of the original modulator structure with an SMF is also shown by a dotted line (when the SSC is not used). It can be observed that by using a tapered SSC, the coupling efficiency can be improved from 41% to 92%, which is a significant improvement. The vertical location of the maximum coupling efficiency is 4 μm lower as the beam has moved downward into the lower waveguide. It can also be noted that

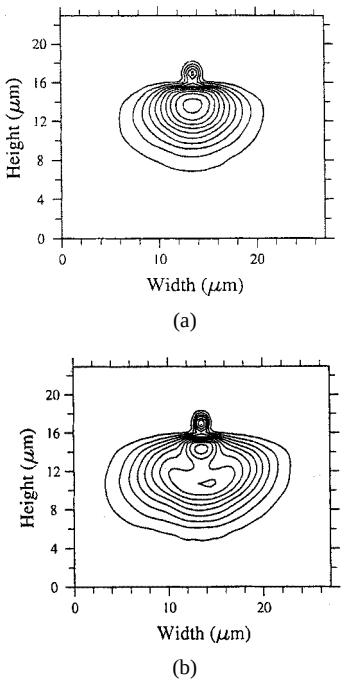

Fig. 12. Output H_y field profile for a 250-μm-long tapered SSC when the final width W_f equals (a) 1.5 μm and (b) 1.0 μm.

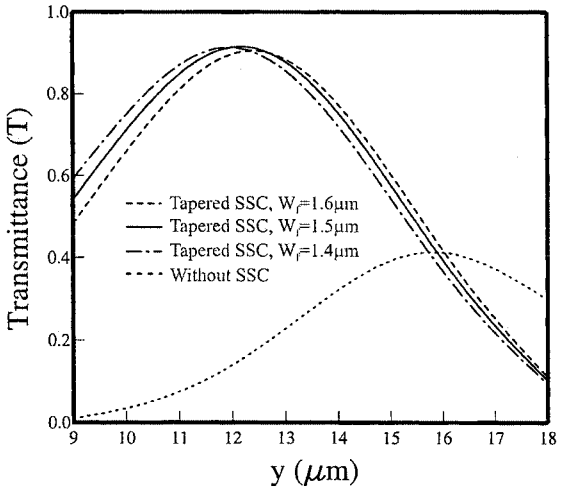

Fig. 13. Variation of the butt-coupling efficiency for a 250-μm-long SSC with the vertical alignment y for different final width W_f.

the -1.0 dB alignment tolerance is about ± 2.0 μm, and such a large coupling tolerance is suitable for direct coupling to a SMF. It should also be noted that the performance characteristics of three spot-size converters, with final widths of 1.4, 1.5, and 1.6 μm, are very close, which indicates that an error of ± 0.1 μm in the fabrication technique would not deteriorate the overall performance of the SSCs designed.

IV. Conclusion

A successful design approach for the implementation of an SSC in a deep-etched semiconductor structure is shown. This approach uses only a laterally tapered primary guide, which is easier to fabricate than one with both a lateral and vertical taper [18]. It is shown that the coupling efficiency can be significantly improved from a mere 41% value (when SSC is not used) to a much more desirable value of 92% (with a loss of only -0.37 dB). The resultant vertical alignment tolerance for -1.0 dB additional loss is more than ± 2.0 μm. It is also demonstrated that a fabrication tolerance of ± 0.1 μm would not deteriorate the expected performance. It can be noted that final taper width should be much less than the value indicated by the modal solutions. However, a much narrower final width W_f, or a sharper taper or its abrupt termination, may produce an unstable or unsuitable optical beam. The excitation of the higher order modes and mode beating along the tapered SSC have also been identified. The tapered designed can be further optimized by using a nonlinear multisegment design for a specific device application.

Acknowledgment

The authors acknowledge valuable discussions with Dr. J. M. Heaton from QinetiQ, Malvern, U.K.

References

[1] M. W. Austin, "Theoretical and experimental investigation of GaAs/GaAlAs and n/n$^+$ GaAs rib waveguides," *J. Lightwave Technology*, vol. 2, pp. 688–694, 1984.

[2] S. -K. Han, R. V. Ramaswamy, W. Q. Li, and P. K. Bhattacharya, "Efficient electro-optic modulator in InGaAlAs/InP optical waveguides," *IEEE Photon. Technol. Lett.*, vol. 5, pp. 46–49, 1993.

[3] J. M. Heaton, M. M. Bourke, S. B. Jones, B. H. Smith, K. P. Hilton, G. W. Smith, J. C. H. Birbeck, G. Berry, S. V. Dewar, and D. R. Wight, "Optimization of deep-etched, single-mode GaAs/AlGaAs optical waveguides using controlled leakage into the substrate," *J. Lightwave Technol.*, vol. 17, pp. 267–281, 1999.

[4] L. H. Spiekman, Y. S. Oei, E. G. Metaal, F. H. Groen, I. Moreman, and M. K. Smit, "Extremely small multimode interference couplers and ultrashort bends on InP by deep etching," *IEEE Photon. Technol. Lett.*, vol. 6, pp. 1008–1010, 1994.

[5] M. Rajarajan, S. S. A. Obayya, B. M. A. Rahman, K. T. V. Grattan, and H. A. El-Mikati, "Characterization of low-loss waveguide bends with offset optimization for compact photonic integrated circuits," *Proc. Inst. Elect. Eng. Optoelectron.*, vol. 147, pp. 382–388, 2000.

[6] J. M. Heaton, R. M. Jenkins, D. R. Wight, J. T. Parker, J. C. H. Birbeck, and K. P. Hilton, "Novel 1-to-N way integrated optical beam splitters using symmetric mode mixing in GaAs/AlGaAs multimode waveguides," *Appl. Phys. Lett.*, vol. 61, pp. 1754–1756, 1992.

[7] C. Themistos and B. M. A. Rahman, "Design issues of a multimode interference-based 3 dB splitters," *Appl. Opt.*, pp. 7037–7044, 2002.

[8] S. S. A. Obayya, S. Haxha, B. M. A. Rahman, C. Themistos, and K. T. V. Grattan, "Optimization of the optical properties of a deeply-etched semiconductor electrooptic modulator," *J. Lightwave Technol.*, vol. 21, pp. 1813–1819, Aug. 2003.

[9] G. A. Vawter, C. T. Sullivan, J. R. Wendt, R. E. Smith, H. Q. Hou, and J. F. Klem, "Tapered rib adiabatic following fiber couplers in etched GaAs materials for monolithic spot-size transformers," *IEEE J. Select. Topics Quantum Electron.*, vol. 3, pp. 1361–1371, 1997.

[10] A. Lestra and J.-Y. Emery, "Monolithic integration of spot-size converters with 1.3-μm lasers and 1.55-μm polarization insensitive semiconductor optical amplifiers," *IEEE J. Select. Topics Quantum Electron.*, vol. 3, pp. 1429–1440, 1997.

[11] K. Kawano, M. Kohtoku, H. Okamoto, Y. Itaya, and M. Naganuma, "Coupling and conversion characteristics of spot-size-converter integrated laser diodes," *IEEE J. Select. Topics Quantum Electron.*, vol. 3, pp. 1351–1360, 1997.

[12] H. Kobayashi, T. Yamamoto, M. Ekawa, T. Watanabe, T. Ishikawa, T. Fujii, H. Soda, S. Ogita, and M. Kobayashi, "Narrow-beam divergence 1.3-μm multiple-quantum-well laser diodes with monolithically integrated tapered thickness waveguide," *IEEE J. Select. Topics Quantum Electron.*, vol. 3, pp. 1384–1391, 1997.

[13] V. Vusirikala, S. S. Saini, R. E. Bartolo, S. Agarwala, R. D. Whaley, F. G. Johnson, D. R. Stone, and M. Dagenais, "1.55-μm InGaAsP-InP laser arrays with integrated-mode expanders fabricated using a single epitaxial growth," *IEEE J. Select. Topics Quantum Electron.*.

[14] B. M. A. Rahman and J. B. Davies, "Finite element solution of integrated optical waveguides," *J. Lightwave Technol.*, vol. LT-2, pp. 682–688, 1984.

[15] B. M. A. Rahman, F. A. Fernandez, and J. B. Davies, "Review of finite element methods for microwave and optical waveguides," *Proc. IEEE*, vol. 79, pp. 1442–1448, 1991.
[16] T. Wongcharoen, B. M. A. Rahman, M. Rajarajan, and K. T. V. Grattan, "Spot-size conversion using uniform waveguide sections for efficient laser-fiber coupling," *J. Lightwave Technol.*, vol. 19, pp. 708–716, 2001.
[17] S. S. A. Obayya, B. M. A. Rahman, and H. El-Mikati, "New full vectorial numerically efficient propagation algorithm based on the finite element method," *J. Lightwave Technol.*, vol. 18, pp. 409–415, 2000.
[18] R. S. Balmer, J. M. Heaton, J. O. Maclean, S. G. Ayling, J. P. Newey, M. Houlton, P. D. J. Calcott, D. R. Wight, and T. Martin, "Vertically tapered epilayers for low-loss waveguide-fiber coupling achieved in a single epitaxial growth run," *J Lightwave Technol.*, vol. 21, pp. 211–217, 2003.

B. M. A. Rahman (S'80–M'82–SM'93) received the B.Sc.Eng. and M.Sc.Eng. degrees in electrical engineering with distinction from the Bangladesh University of Engineering and Technology (BUET), Dhaka, Bangladesh, in 1976 and 1979, respectively, receiving two gold medals for being the best undergraduate and graduate student of the university in these two years. In 1979, he was awarded with a Commonwealth Scholarship to study for the Ph.D. degree in the U.K. and, subsequently, in 1982, received the Ph.D. degree in electronics from University College London, London, U.K.

From 1976 to 1979, he was a Lecturer at the Electrical Engineering Department, BUET. In 1982, after receiving the Ph.D. degree, he joined University College London as a Postdoctoral Research Fellow and continued his research work on the development of the finite-element method for characterizing optical guided-wave devices. In 1988, he joined City University, London, U.K., as a Lecturer. Currently, he is Professor and Assistant Dean of Engineering. At City University, he leads the research group on photonics modeling, specializing in the use of rigorous and full-vectorial numerical approaches to design, analyze, and optimize a wide range of photonic devices. He has published more than 250 journal and conference papers, and his journal papers have been cited nearly 800 times.

Prof Rahman is a Member of the Institution of Electrical Engineers (IEE), London, U.K., and the European Optical Society and is a Chartered Engineer.

W. Boonthittanont, photograph and biography not available at the time of publication.

S. S. A. Obayya, photograph and biography not available at the time of publication.

T. Wongcharoen, photograph and biography not available at the time of publication.

E. O. Ladele, photograph and biography not available at the time of publication.

K. T. V. Grattan, photograph and biography not available at the time of publication.